



This open access document is published as a preprint in the Beilstein Archives with doi: 10.3762/bxiv.2019.154.v1 and is considered to be an early communication for feedback before peer review. Before citing this document, please check if a final, peer-reviewed version has been published in the Beilstein Journal of Nanotechnology.

This document is not formatted, has not undergone copyediting or typesetting, and may contain errors, unsubstantiated scientific claims or preliminary data.

Preprint Title The influence of the magnetic nanoparticles coating from colloidal system on the magnetic relaxation time

Authors Mihaela Osaci and Matteo Cacciola

Publication Date 06 Dez 2019

Article Type Full Research Paper

ORCID® iDs Mihaela Osaci - <https://orcid.org/0000-0003-4062-7556>

The influence of the magnetic nanoparticles coating from colloidal system on the magnetic relaxation time

Mihaela Osaci*

“Politehnica” University of Timisoara,
Department of Electrical Engineering and Industrial Informatics,
2 Victoriei Square, 300006 Timisoara, Timis County, Romania

*corresponding author, email: mihaela.osaci@fih.upt.ro

Matteo Cacciola

Cooperativa TEC, Via Nazionale, n. 439, I-89134 Pellaro di Reggio Calabria

Abstract

Currently, the colloidal systems of monodomain superparamagnetic nanoparticles are used in biomedical applications, such as hyperthermia treatment for cancer. In this type of colloid, called nanofluid, there is a tendency of nanoparticle agglomeration. It has been shown experimentally that the nanoparticle coating plays an important role in the nanoparticle dispersion stability and biocompatibility, which role was theoretically understudied so far. Also, the implications of nanoparticle coating on the magnetic properties of the nanoparticles have been little studied. This paper presents the theoretical study, by numerical simulation, on how the nanoparticle coating affects the tendency of agglomeration of the nanoparticles and the Néel relaxation time – or the effective magnetic relaxation time of the system. For simulating the self-organization of colloidal nanoparticles, we apply a Langevin dynamics stochastic method based on an effective Verlet-type algorithm, and the Néel magnetic relaxation time is assessed through the Coffey method in oblique magnetic field, adapted to the local magnetic field on a nanoparticle.

Keywords: magnetic nanoparticles coating, colloidal system, magnetic relaxation time, simulation, Langevin dynamics stochastic method, effective Verlet-type algorithm

Introduction

One of the most important biomedical applications of the colloidal magnetic nanoparticle systems is the magnetic hyperthermia as an alternative cancer treatment. The magnetic nanoparticles, after reaching the tumour, are locally subjected to an alternative magnetic field and they generate heat that kills the cancer cells [1], in general through two phenomena: Néel relaxation (internal phenomenon, i.e. rotation of the particle magnetic moment inside the particle) and Brown relaxation (external phenomenon, i.e. rotation of the nanoparticle along with the magnetic moment). Both internal and external sources of “friction” lead to a delay phase in the orientation of the particle magnetic moments in the direction of the applied magnetic field, thus generating heat. This heat increases the temperature of the tumour cell and, ultimately, kills it [1- 4].

The magnetic nanoparticles, currently studied intensely for applications in magnetic hyperthermia, are iron oxide nanoparticles, in particular magnetite (Fe_3O_4) and maghemite ($\gamma\text{-Fe}_2\text{O}_3$), due to the possibilities of obtaining them in small dimensions for their reduced toxicity and possibilities of easy functionalization of their surfaces. Some of the methods currently used to synthesize these nanoparticles are: the modified sol-gel method used to prepare nanoparticles of nanometric size under supercritical conditions of ethyl alcohol and alkaline co-precipitation, with an additional step of a hydrothermal method or thermal decomposition technique. We mention that the method of obtaining nanoparticles by thermal decomposition of an iron precursor in the presence of NaBH_4 in a polyol was found suitable for size control in both chemical approaches [1, 5].

Because certain technological procedures for the synthesis of these nanoparticles can affect their quality in terms of dimensions, chemical composition and crystalline structure, the attention is

now directed towards improving their production quality. In this respect, Plackett-Burman design of experiments is a filtration analysis used in the initial investigation of the main effects of the factors on a characteristic of the final material [6].

It can be shown experimentally that the uncoated superparamagnetic nanoparticles are difficult to synthesize, they cannot maintain stability in a colloidal suspension and, therefore, they are difficult to use in the magnetic hyperthermia therapy [7].

By exposing the nanoparticles to the acidic environments of the living organisms, certain processes of structural degradation caused by corrosion on the nanoparticle surfaces occur. This biodegradation in acidic media leads over time to significant modification of the magnetic properties of the nanoparticles [8]. These arguments are required to support the need to cover the nanoparticles. The coating of nanoparticles is made for: reducing the nanoparticle surface sensitivity to air, humidity and acidity, subsequent functionalization and absorption of proteins, creation of surface hydrophilic molecules to prevent nanoparticle agglomeration, reduction of capillary obstruction risk, and improving the blood circulation for nanoparticle transport in the targeted area, preservation of the physical-chemical properties of the nanoparticles, prevention of nanoparticle opsonization by the reticuloendothelial system that would cause their fast flowing from the bloodstream before reaching the target and making a biocompatible and non-toxic shield around the nanoparticles, because their surface is in direct contact with the blood and tissues. The thickness of the nanoparticle coating can increasingly affect the magnetic properties, as well as the hyperthermia.

The materials used as a coating agent for the magnetic nanoparticles can be organic or inorganic. The inorganic coating causes the surface of the nanoparticles to bind the biological ligands, while maintaining the nanoparticle stability. The organic coating, in particular the polymer, has a number of advantages, such as: better particle dispersion, good colloidal stability, biocompatibility, good nanoparticle circulation in the blood, reduced toxicity and low risk of blood capillary obstruction.

In the recent years, a new class of nanofluids with biomedical applications, which are ultrastable and often biocompatible, have been developed using a combination of electrostatic and steric stabilisation methods [9]. Despite these stabilization methods, a number of recent papers have experimentally shown a tendency to agglomeration, even in the absence of an external magnetic field [10, 11]. This could be a problem when using ferrofluids for medical applications: the nanoparticle agglomeration and sedimentation can create thrombi inside the blood vessels [12].

The control of agglomeration is becoming essential to improve the applicability of the magnetic nanoparticles. In this regard, the optimized microemulsion method can be used to obtain homogenous silica coatings on the $\text{Fe}_{3-x}\text{O}_4$ nanoparticles [13]. It shows that the thickness of this coating layer is controlled almost at will allowing much higher average separation among particles as compared to the oleic acid coating present on pristine NPs [13].

Homogeneous, spherical polymer-coated magnetite nanoparticles have been successfully prepared, showing a superparamagnetic response of the synthesized MNPs. The polymer coating has been demonstrated to provide extra stability of the MNPs in aqueous media [14]. For better biocompatibility or for specific hydrophilic properties, in most cases the nanoparticles are coated with a polymer layer, such as the polyethylene glycol (PEG) [15].

The experimental data on the nanoparticle coating influence on their magnetic properties are quite controversial. Recently, in situ reduction method applied for core-shell Fe_3O_4 with Ag and polyacrylic acid indicated that the thin polymer coating layer had a great influence in enhancing the hyperthermia efficiency [16]. Zavisova et al. [17] prepared and experimentally investigated the Fe_3O_4 nanoparticles with different protein or polymer outer shell. They found no correlation between the coating layer thickness and the magnetic hyperthermia specific adsorption rate.

The issues mentioned in the previous paragraph show the need for research on the influence of the coating on the magnetic behaviour of the nanoparticles, as other authors pointed out in their work (e.g. [7]). To meet these needs, the current paper aims to use certain simulation models to study the

influence of nanoparticle coating on the tendency of nanoparticle agglomeration and on the Néel magnetic relaxation time and, respectively, on the effective magnetic relaxation time.

Results and Discussion

Simulation methods used in the study

For numerical simulation, we start from a single-domain system, made of spherical iron oxide nanoparticles, with a lognormal distribution of the grain sizes. Each nanoparticle is composed of a magnetic core and a nonmagnetic surface layer of stabilizing surfactant. The system temperature is considered constant.

For numerical simulation, two models developed by the authors and widely presented in the specialized literature have been used [18- 20].

For self-organization of the colloidal magnetic nanoparticles simulation, we used the Langevin dynamics stochastic method based on an effective Verlet-type algorithm [18].

The Néel magnetic relaxation time is assessed through the Coffey method in oblique magnetic field, adapted to the local magnetic field on a nanoparticle [20- 21].

Method for self-organization of colloidal magnetic nanoparticles simulation

This method starts from numerical solutions of the Langevin equations for the translational and rotational motions of an i^{th} nanoparticle in the basic liquid [18].

The forces acting among the nanoparticles of the system, i.e. the Van der Waals forces, the electrostatic repulsive forces, the magnetic dipolar forces, the steric repulsion forces have to be taken into account for the coated nanoparticles and the random Brownian force [18, 22-25]. The stabilisation of magnetic particles can be achieved by two repulsive forces: electrostatic and steric repulsion [18], [22-23]. Besides the random Brownian torque, the conservative torque acting on the nanoparticle is a magnetic torque. The random Brownian force and torque are usually modelled using the Gaussian noise [20-21].

For solving numerically the equations of motion, we use the effective Verlet-type algorithm [18 - 19].

The Coffey method in oblique magnetic field, adapted to the local magnetic field on a nanoparticle

In general, in the literature, the evaluation of the Néel relaxation time is made using the Néel-Brown model [26], [27], valid if the nanoparticles do not interact magnetostatically one with the other one. If the magnetic dipolar interaction among the nanoparticles is not neglected, this model leads to a rather unrealistic approximation [20].

The dipolar magnetic field on the nanoparticle and the external magnetic field create a resultant for internal magnetic field \vec{H}_i^J on a nanoparticle, field that does not generally act along the direction of easy magnetisation axis of the nanoparticle, being a so-called oblique magnetic field [21].

The nanoparticle Néel relaxation time in oblique magnetic fields is [20-21]:

$$\tau_N^i = \frac{4\pi\tau^i v_i M_s (S_{i1}^{-1} + S_{i2}^{-1})}{\left(\sqrt{c_{i1}^{(1)} c_{i2}^{(1)}} \cdot e^{-\Delta E_{i12}} + \sqrt{c_{i1}^{(2)} c_{i2}^{(2)}} \cdot e^{-\Delta E_{i21}} \right)} \quad (1)$$

where ΔE_{i12} and ΔE_{i21} are the normalized energy barriers for magnetic moment re-orientations. The free diffusion time of magnetisation τ_{ON}^i for low damping is [20-21]:

$$\tau_{ON}^i = \frac{v_i M_s}{2\gamma\alpha k_B T} \quad (2)$$

where v_i is the volume of the i^{th} nanoparticle, M_s the spontaneous magnetisation, k_B the Boltzmann constant, T the temperature, α the damping constant and γ the gyromagnetic ratio.

In Eq. (1):

$$c_{i1}^{(p)} = 2\sigma_i (\cos 2\theta_{ip} + h_i \cos(\theta_{ip} - \psi_i)), c_{i2}^{(p)} = 2\sigma_i (\cos^2 \theta_{ip} + h_i \cos(\theta_{ip} - \psi_i)), \text{ with } p = 1, 2 \quad (3)$$

$$\sigma_i = \frac{K_i^{eff} v_i}{k_B T} \quad (4)$$

with Ψ_i the angle between \vec{H}_i and the easy anisotropy axis of the i^{th} nanoparticle. θ_{ip} are the solutions of the transcendental equation:

$$\sin 2\theta_i = 2h_i \sin(\Psi_i - \theta_i) \quad (5)$$

In (5) θ_i is the angle between magnetisation and easy anisotropy axis of the i^{th} nanoparticle.

$$h_i = \frac{\mu_0 M_s H_i}{2K_i^{eff}} \quad (6)$$

In Eq. (4) and (6) K_i^{eff} effective magnetic anisotropy constant of the i^{th} nanoparticle.

If $h_i < h_{ic}(\Psi_i) < 1$ [20-21]:

$$\begin{aligned} \cos\theta_{i1,2} = \pm \mu \frac{h_i^2}{2} \sin^2 \psi_i + h_i^3 \sin^2 \psi_i \cos \psi_i \mu \frac{h_i^4}{16} (13 + 11 \cos 2\psi_i) \sin^2 \psi_i + \frac{h_i^5}{2} (3 + \cos 2\psi_i) \sin^2 \psi_i \cos \psi_i \mu \\ \mu \frac{h_i^6}{64} (183 + 156 \cos 2\psi_i - 19 \cos 4\psi_i) \sin^2 \psi_i + \dots \end{aligned} \quad (7)$$

$$\begin{aligned} \Delta E_{i12} = \sigma_i [1 - 2h_i (\sin \Psi_i - \cos \Psi_i) + h_i^2 + \frac{h_i^3}{2} \sin 2\Psi_i (\cos \Psi_i - \sin \Psi_i) + \frac{h_i^4}{2} \sin^2 2\Psi_i + \\ + \frac{h_i^5}{32} \sin 2\Psi_i (7 \cos \Psi_i - 3 \cos 3\Psi_i - 7 \sin \Psi_i - 3 \sin 3\Psi_i) + \frac{h_i^6}{2} \sin^2 2\Psi_i + \dots] \end{aligned} \quad (8)$$

$$\begin{aligned} \Delta E_{i21} = \sigma_i [1 - 2h_i (\sin \Psi_i + \cos \Psi_i) + h_i^2 + \frac{h_i^3}{2} \sin 2\Psi_i (\cos \Psi_i + \sin \Psi_i) + \frac{h_i^4}{2} \sin^2 2\Psi_i + \\ + \frac{h_i^5}{32} \sin 2\Psi_i (7 \cos \Psi_i - 3 \cos 3\Psi_i + 7 \sin \Psi_i + 3 \sin 3\Psi_i) + \frac{h_i^6}{2} \sin^2 2\Psi_i + \dots] \end{aligned} \quad (9)$$

$$\begin{aligned} S_{i1,2} = \sigma_i \sqrt{h_i \sin \Psi_i} [16 - \frac{104}{3} h_i \sin \Psi_i + h^2 (1 - 21 \cos 2\Psi_i) + \frac{h_i^3}{2} \sin \Psi_i (45 + 51 \cos 2\Psi_i) + \dots] \pm \\ \pm 2\pi \sigma_i h_i^2 \sin 2\Psi_i (4 - 3h_i \sin \Psi_i - 2h_i^2 \sin^2 \Psi_i + \dots) \end{aligned} \quad (10)$$

Simulation conditions and results

For this study, we consider the case of a colloid with electrosteric stabilisation. The system comprises 50 spherical magnetite nanoparticles with spontaneous magnetisation of $M_s = 4.46 \cdot 10^5$ A/m, whose sizes have a lognormal distribution, which are dispersed in water whose dynamic viscosity is $8.9 \cdot 10^{-4}$ Pa·s and the relative electrical permittivity is 78.5. The Hamaker constant for magnetite in water is $39 \cdot 10^{-20}$ J [19]. The temperature is 298 K, the coating layer thickness ranges from 1 nm to 3

nm, the ion concentration in solution is 10^{26} ions/m³, their valence is 1, the surface density of the polymers ξ ranges from 10^{16} m⁻² to $4.5 \cdot 10^{17}$ m⁻², and the surface charge is $1.6 \cdot 10^{-15}$ C. The average diameter of the nanoparticles is $d_m = 10$ nm, with a standard deviation of $0.1 \cdot d_m$. We consider that the volume fraction of the nanoparticles is 0.05. We set the external magnetic field intensity to the value of 15kA/m along the Z-axis.

It is initially considered a random arrangement the nanoparticles in face-centred cubic grid. With Langevin dynamics stochastic method, it is obtained an aggregate structure. For example, the Figures 1-2 show the positions of nanoparticles inside the test cube a) at the initial moment and b) after 0.1ms (Figure 1 - the coating layer thickness is 1 nm and the surface density of the polymers $\xi = 10^{16}$ m⁻², Figure 2 - the coating layer thickness is 1 nm and the surface density of the polymers $\xi = 4.5 \cdot 10^{17}$ m⁻²).

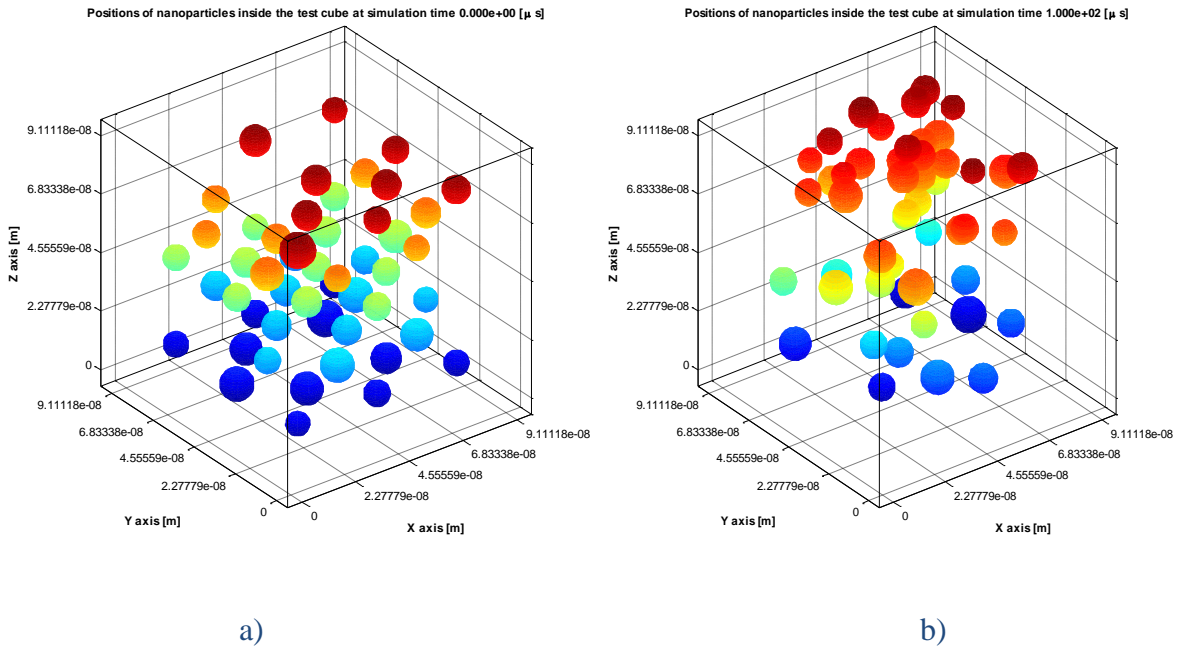


Fig. 1 - Positions of nanoparticles inside the test cube in a) initial moment and b) after 0.1ms (the coating layer thickness is 1 nm, and the surface density of the polymers $\xi = 10^{16}$ m⁻²)

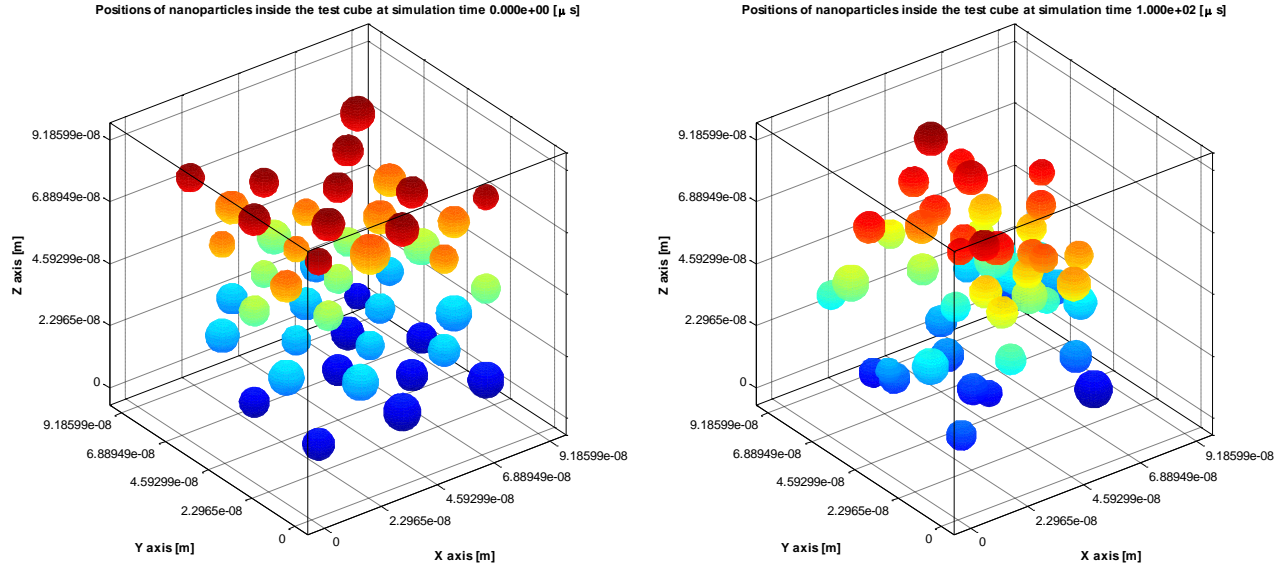


Fig. 2 - Positions of nanoparticles inside the test cube in a) initial moment and b) after 0.1ms (the coating layer thickness is 1 nm, and the surface density of the polymers $\xi = 4.5 \cdot 10^{17} \text{ m}^{-2}$)

We can see in the figures 1 and 2, that the polymer concentration in the nanoparticle coating influences the aggregate structure of the nanoparticles.

After obtaining the aggregate structure of the nanoparticles, by using the Coffey method in oblique magnetic field, adapted to the local magnetic field on a nanoparticle, we can find, for each nanoparticle, the Néel relaxation times τ_N^i . For each nanoparticle, the effective magnetic relaxation time can be described as follows [27]:

$$\frac{1}{\tau_{eff}^i} = \frac{1}{\tau_N^i} + \frac{1}{\tau_B^i} \quad (11)$$

where τ_B^i is the Brownian relaxation time. The Brownian process represents the nanoparticle rotation in the fluid environment. For spherical particles, the Brownian relaxation time is usually described by:

$$\tau_B^i = \frac{3v_H^i \eta}{k_B T} \quad (12)$$

where v_H is the hydrodynamic volume of the particle, and η is the coefficient of dynamic viscosity.

Having for each nanoparticle the value of the effective magnetic relaxation time, we can calculate the average effective magnetic relaxation time.

The relaxation mechanism which dominates the magnetic behaviour of the colloidal suspensions is determined by the nanoparticle properties. For nanoparticles of 10 nm in diameter, it can be shown that the Néel relaxation process is dominant (Figures 3, 4).

To study how the nanoparticle coating layer thickness and the polymer surface density influence the magnetic behaviour of the nanoparticles, for different values of the polymer surface density, we will vary the nanoparticle coating layer thickness between 1 nm and 3 nm. Then, for each thickness of the coating layer, we will vary the polymer surface density between 10^{16} m^{-2} and $4.5 \cdot 10^{17} \text{ m}^{-2}$. The results are shown in Figures 3 and 4 a) and b). As can be seen in Figures 3 and 4, the average Néel relaxation time and, respectively, the average effective magnetic relaxation time, are affected either by the thickness of the nanoparticle coating layer or by the density of the polymer surface layer.

The Figures 3a) and b) show the average Néel relaxation time and, respectively, the average effective magnetic relaxation time versus the nanoparticle coating layer thickness, at different values of the polymer surface density.

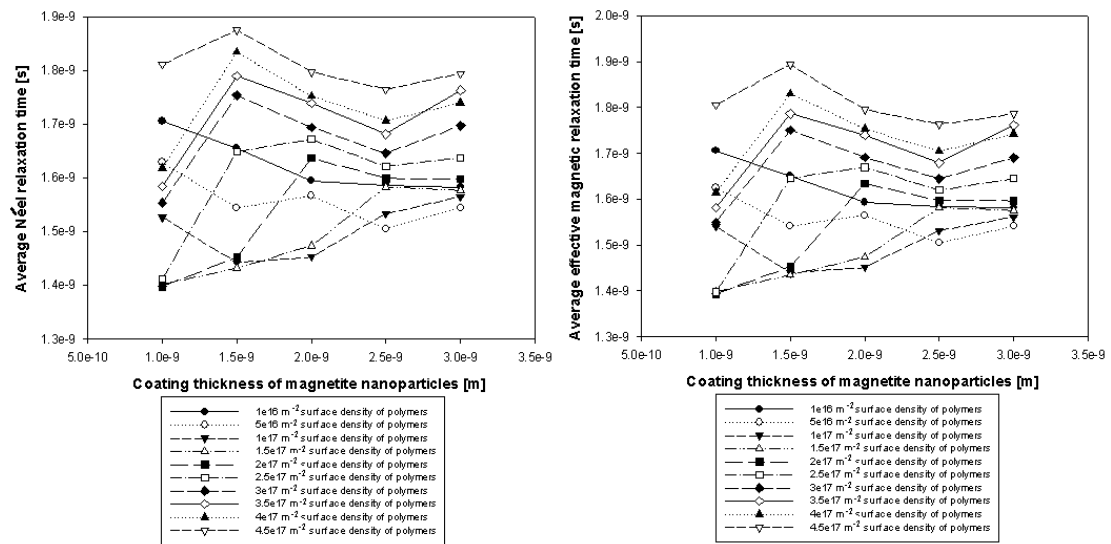


Fig. 3 Average Néel relaxation time (a) and average effective magnetic relaxation time (b)

versus the nanoparticle coating layer thickness, at different values of the polymer surface density

In the Figures 3a) and b), we can see that, for low values of the polymers surface density in the nanoparticle coating layer (10^{16} m^{-2} and $5 \cdot 10^{16} \text{ m}^{-2}$, respectively), the average Néel relaxation time (a) and the average effective magnetic relaxation time (b) decreases with increasing layer thickness. At values of about 10^{17} m^{-2} of the polymer surface density, the average Néel relaxation time (a) and the average effective magnetic relaxation time (b) increases with decreasing coating layer thickness, reaches a minimum value, followed by a slight increase. At high values of the polymer surface density, the average Néel relaxation time (a) and the average effective magnetic relaxation time (b) increases with increasing coating layer thickness, reaches a maximum value, followed by a slight decrease. The obtained results can be explained by the competition between the attraction forces, especially the magnetic dipolar interaction forces, directly proportional to the magnetic moments of the particles and inversely proportional to the 5th power of the interparticle distances and the forces of rejection, especially the steric forces directly proportional to the thickness of the surfactant coating layer. At low values of the polymer surface density, the action of the rejection forces, in particular of the steric forces, is weaker, and the forces of attraction predominate, especially the magnetic dipolar interaction forces acting among the nanoparticles. As such, there is a tendency of agglomeration, which means large local volumetric concentrations of large nanoparticles. At high values of the polymer surface density, the action of the rejection forces, in particular the steric forces, is stronger, to the detriment of the attraction forces, especially the forces of magnetic dipolar interaction acting among the nanoparticles, which results in smaller local nanoparticle concentrations. In the extreme points (minimum, maximum), an unstable balance is established between the forces of rejection and the forces of attraction. Regarding the magnetic behaviour of the superparamagnetic nanoparticle system, the literature shows a relaxation time decrease with increasing interparticle interaction in the case of diluted systems [28-31]. On the other hand, it is claimed that the relaxation time increases when the particle concentration increases [32-33].

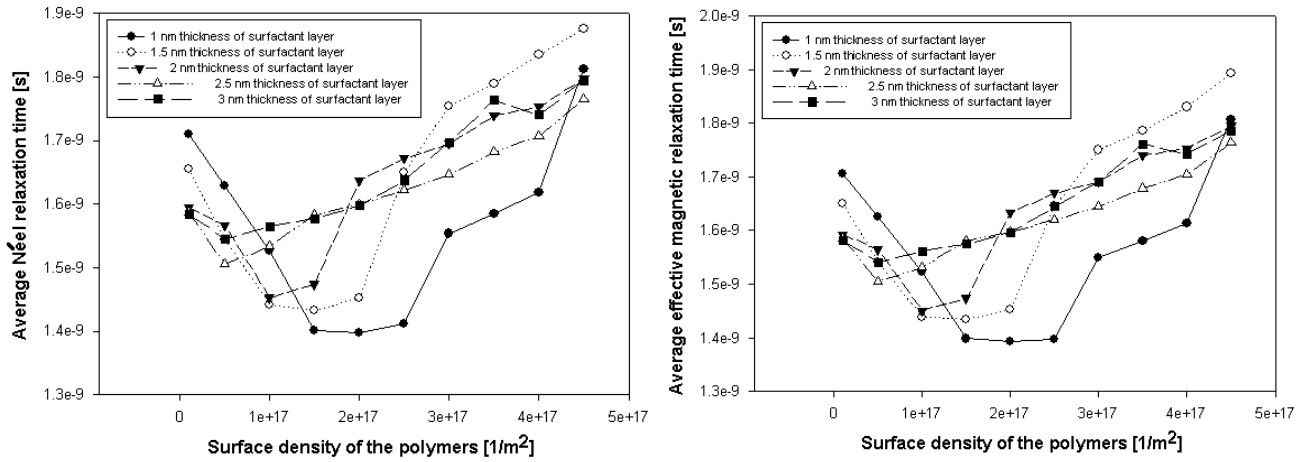


Fig. 4 Average Néel relaxation time (a) and average effective magnetic relaxation time (b) versus polymer surface density, at different values of the nanoparticle coating layer thickness

The Figures 4a) and b) show the Néel relaxation time and the effective magnetic relaxation time versus the polymer surface density, at different thicknesses of the nanoparticle coating layer. Regardless of the coating layer thickness, for low values of the polymer surface density, the average Néel relaxation time and, respectively, the average effective magnetic relaxation time decreases with increasing polymer surface density, reaches a minimum value, and then, at high values of the polymer surface density, there is an increase in the average Néel relaxation time and, respectively, in the average effective magnetic relaxation time. The minimum value of the average Néel relaxation time, as well as the minimum value of the average effective magnetic relaxation time, is higher and higher as the nanoparticle surfactant coating layer is thicker. For relatively small thicknesses of the nanoparticle coating layer, the minimum value of the average Néel relaxation time, as well as the minimum value of the average effective magnetic relaxation time, moves to small values of the polymer surface density, as the thickness of the surfactant coating layer of the magnetic nanoparticles increases. For large thicknesses, this displacement is almost unnoticeable. This complicated dependence can also be explained by the competition between the rejection forces, in particular the steric rejection forces, and

the attraction forces, in particular the magnetic dipolar interaction forces acting among the nanoparticles.

Conclusions

In this paper, two simulation models are used to understand how the surfactant coating layer thickness and, respectively, the polymer surface layer density, are influencing the Néel relaxation time and, respectively, the effective magnetic relaxation time, in a system of magnetic nanoparticles suspended in a liquid matrix. So, for simulating the self-organization of the colloidal nanoparticles, we used a Langevin dynamics stochastic method based on an effective Verlet-type algorithm, and for the Néel relaxation time simulation we used the Coffey solution in oblique magnetic field adapted to the local magnetic field on the nanoparticle, relation (1). The effective magnetic relaxation time was calculated based on the relation (11).

Following the numerical simulations, it was revealed that the average Néel relaxation time and, respectively, the average effective magnetic relaxation time, are affected either by the surfactant coating layer thickness or by the polymer surface layer density.

More specifically, for small values of the polymer surface layer density in the nanoparticle coating, the average Néel relaxation time and, respectively, the average effective magnetic relaxation time decreases with increasing coating thickness. At intermediate values of the polymer surface layer density, the average Néel relaxation time and, respectively, the average effective magnetic relaxation time decreases with increasing the thickness of the coating, reaches a minimum value, after which a slight increase occurs. At high values of the polymer surface layer density, the average Néel relaxation time and, respectively, the average effective magnetic relaxation time increases with increasing the thickness of the coating, reaches a maximum value, after which a slight decrease occurs.

It was also revealed that, regardless of the thickness of the coating, for small values of the polymer surface layer density, the average Néel relaxation time and, respectively, the average effective

magnetic relaxation time decreases with the increase of the polymer surface layer density, reaches a minimum value, after which, at high values of the polymer surface layer density, we notice an increase of the average Néel relaxation time, as well of the average effective magnetic relaxation time. The minimum value of the average Néel relaxation time and, respectively, the average effective magnetic relaxation time, is higher and higher when the thickness of the nanoparticle surfactant coating is increasing. For relatively small thicknesses of the nanoparticle coating layer, the minimum value of the average Néel relaxation time and, respectively, of the average effective magnetic relaxation time, moves to low values of the polymer surface density when the thickness of the surfactant coating of the magnetic nanoparticles increases. For large thicknesses, this displacement is almost unnoticeable.

All these behaviours of the average Néel relaxation time and, respectively, of the average effective magnetic relaxation time, can be explained by the competition between the rejection forces and the attraction forces acting among the nanoparticles.

The results presented in this paper are of real help for various applications of the colloidal magnetic nanoparticle systems, in particular biomedical applications [34-39], such as magnetic hyperthermia with nanoparticles, which are of great interest either theoretically or applicatively, being a possible alternative in the therapy of cancer in its various stages and forms.

References

- [1] Pala, J.; Mehta, H.; Mandaliya, R.; Moradiya, M.; Savaliya, C.R.; Markna J.H. Tailoring of magnetic hyperthermia treatment using superparamagnetic iron oxide nanoparticles. *Mol. Biol. Med.* **2017**, 2(1), 174-175.
- [2] Usov, N. A.; Nesmeyanov, M. S.; Tarasov, V. P. Magnetic Vortices as Efficient Nano Heaters in Magnetic Nanoparticle Hyperthermia. *Sci. Rep.* **2018**, 8, 1224

- [3] Maier-Hauff, K. et al. Efficacy and safety of intratumoral thermotherapy using magnetic iron-oxide nanoparticles combined with external beam radiotherapy on patients with recurrent glioblastoma multiforme. *J. Neuro-oncol.* **2011**, 103, 317-324
- [4] Johannsen, M.; Thiesen, B.; Wust, P.; Jordan, A. Magnetic nanoparticle hyperthermia for prostate cancer. *Int. J. Hyperthermia.* **2010**, 26, 790–795
- [5] Kotoulas, A.; Dendrinou-Samara, C.; Angelakeris, M.; Kalogirou, O. The Effect of Polyol Composition on the Structural and Magnetic Properties of Magnetite Nanoparticles for Magnetic Particle Hyperthermia. *Materials.* **2019**, 12(17), 2663
- [6] Rost, N. C. V. ; Broca, F. M. ; Gonçalves, G. C.; Cândido, M. A.; Castilho, M. L. ; Raniero, L. J. Synthesis of Iron Oxide Nanoparticles Optimized by Design of Experiments. *Braz. J.Phys.* **2019**, 49(1), 22-27
- [7] Hedayatnasab, Z.; Abnisa, F.; Wan Daud, W.M.A. Investigation properties of superparamagnetic nanoparticles and magnetic field-dependent hyperthermia therapy. *IOP Conf. Series: Materials Science and Engineering.* **2018**, 334, 012042
- [8] Lartigue, L. et al. Biodegradation of Iron Oxide Nanocubes: High-Resolution In Situ Monitoring. *ACS Nano.* **2013**, 7, 3939-3952
- [9] Heinrich, D.; Goñi, A.R.; Thomsen, C. Dynamics of magnetic-field-induced clustering in ionic ferrofluids from Raman scattering. *J.Chem. Phys.* **2007**, 126, 124701
- [10] Sanz, B.; Calatayud, M.P.; Cassinelli, N.; Ibarra, M.R.; Goya, G.F. Long-Term Stability and Reproducibility of Magnetic Colloids are Key Issues for Steady Values of Specific Power Absorption Over Time. *Eur. J. Inorg. Chem.* **2015**, 2015(27), 4524-4531
- [11] Etheridge, M.L.; Hurley, K.R.; Zhang, J.; Jeon, S.; Ring, H.L.; Hogan, C.; Haynes, C.L.; Garwood, M.; Bischof, J.C. Accounting for biological aggregation in heating and imaging of magnetic nanoparticles. *Technology (Singap World Sci).* **2014**, 2(3), 1-15

- [12] Dutz S.; Hergt, R. Magnetic particle hyperthermia - a promising tumour therapy?, *Nanotechnology*. **2014**, 25, 452001-452029
- [13] Pérez, N.; Moya, C.; Tartaj, P.; Labarta, A.; Batlle, X. Aggregation state and magnetic properties of magnetite nanoparticles controlled by an optimized silica coating. *J. Appl.Phys.* **2017**, 121(4), 044304
- [14] Reyes-Ortega, F.; Delgado, Á. V.; Schneider, E.K.; Fernández, B.L.C.; Iglesias, G.R. Magnetic Nanoparticles Coated with a Thermosensitive Polymer with Hyperthermia Properties. *Polymers*. **2018**, 10(1), 10
- [15] Dabbagh, A.; Hedayatnasab, Z.; Karimian, H.; Sarraf, M.; Yeong, C.H.; Madaah Hosseini, H.R.; Abu Kasim, N.H.; Wong, T.W.; Rahman, N.A. Polyethylene glycol-coated porous magnetic nanoparticles for targeted delivery of chemotherapeutics under magnetic hyperthermia condition. *Int. Journal Hyperthermia*. **2018**, 14,1-11
- [16] Ding, Q.; Liu, D.; Guo, D.; Yang, F.; Pang, X.; Che, R.; Zhou, N.; Xie, J.; Sun, J.; Huang, Z.; Gu, N. Shape-controlled fabrication of magnetite silver hybrid nanoparticles with high performance magnetic hyperthermia. *Biomaterials*. **2017**, 124, 35-46
- [17] Zavisova, V.; Koneracka, M.; Gabelova, A.; Svitkova, B.; Ursinyova, M.; Kubovcikova, M.; Antal, I.; Khmara, I.; Jurikova, A.; Molcan, M.; Ognjanović, M.; Antić, B.; Kopcansky, P. Effect of magnetic nanoparticles coating on cell proliferation and uptake. *J. Magn. Magn. Mater.* **2019**, 472, 66-73
- [18] Osaci, M.; Cacciola, M. Study about the nanoparticle agglomeration in a magnetic nanofluid by the Langevin dynamics simulation model using an effective Verlet-type algorithm. *Microfluid. Nanofluid.* **2017**, 21(2)
- [19] Grønbech-Jensena, N.; Faragoa, O. A simple and effective Verlet-type algorithm for simulating Langevin dynamics. *Mol. Phys.* **2013**, 111(8), 983–991

- [20] Osaci, M.; Cacciola, M. An adapted Coffey model for studying susceptibility losses in interacting magnetic nanoparticles. *Beilstein J. Nanotech.* **2015**, 6(1), 2173–2182
- [21] Coffey, W. T.; Crothers, D. S. F.; Dormann, J. L.; Geoghegan, L. J.; Kalmykov, Yu. P., Waldron, J. T.; Wickstead, A. W. Effect of an oblique magnetic field on the superparamagnetic relaxation time. *Phys. Rev.* **1995**, B 52, 15951
- [22] Polyakov, A. Yu; Lyuty, T.V.; Denisov, S.; Reva, V.V.; Hånggi, P. Large-scale ferrofluid simulations on graphics processing units. *Comput.Phys. Commun.* **2013**, 184, 1483-1489
- [23] Glotzer, S.C.; Solomon, M.J.; Kotov, N.A. Self-Assembly: From Nanoscale to Microscale Colloids. *AICHE J.* **2004**, 50(12), 2978-2985
- [24] Laurent, S.; Forge, D.; Port, M.; Roch, A.; Robic, C.; Elst, L.V.; Muller, R. N. Magnetic Iron Oxide Nanoparticles: Synthesis, Stabilization, Vectorization, Physicochemical Characterizations, and Biological Applications. *Chem. Rev.* **2008**, 108, 2064–2110
- [25] Ghosh, S.; Jiang, W.; McClements, J.D., Xing, B.S. Colloidal Stability of Magnetic Iron Oxide Nanoparticles: Influence of Natural Organic Matter and Synthetic Polyelectrolytes. *Langmuir.* **2011**, 27 (13), 8036-8043
- [26] Brown, W. F. Jr. Thermal Fluctuations of a Single-Domain Particle. *Phys. Rev.* **1963**, 130 1677-1686
- [27] Coffey, W.T.; Gregg, P.J.; Kalmzkov, Yu.P. *On the theory of Debye and Néel relaxation of single domain ferromagnetic particles: Advances in Chemical Physics.* Prigogine, I.; Rice, S. A. John Wiley & Sons, Inc., Hoboken, NJ: USA, 1992
- [28] Hansen, M.F.; Morup, S. Models for the dynamics of interacting magnetic nanoparticles, *J. Magn. Mater.* **1998**, 184, 262-274
- [29] Prené, P.; Tronc, E.; Jolivet, J.P.; Livage, J.; Cherkaoui, R.; Noguès, M.; Dormann, J.L.; Fiorani, D. *IEEE Trans. Magn.* **1993**, 29, 2658
- [30] Mørup, S.; Tronc, E. *Phys. Rev. Lett.* **1994**, 72, 3278

- [31] Jiang, J.Z.; Morup, S.; Jonsson, T.; Svedlindh, P. in I. Ortalli (Ed.), Proc. ICAME'95, SIF: Bologna, 1996, pp. 529
- [32] Dormann, J.L.; Bessais, L.; Fiorani, D. J. A dynamic study of small interacting particles: superparamagnetic model and spin-glass laws. *Phys. C: Solid State Phys*, **1988**, 21, 2015-2034
- [33] Dormann, J.L.; Spinu, L.; Tronc, E.; Jolivet, J.P.; Lucari, F.; D'Orazio, F.; Fiorani, D. Effect of interparticle interactions on the dynamical properties of γ -Fe₂O₃ nanoparticles. *J. Magn. Magn. Mater.* **1998**, 183, 255-260
- [34] Adedoyin, A. A.; Ekenseair, A. K. Biomedical applications of magneto-responsive scaffolds. *Nano Res.* **2018**, 11(10), 5049–5064
- [35] Kumar, S.; Kumari, P.; Singh, R. Emerging Nanomaterials for Cancer Therapy. *Nanoparticles in Medicine.* **2019**, pp. 25-54
- [36] Chao, Y.; Chen, G.; Liang, C.; Xu, J.; Dong, Z.; Han, X.; Wang, C.; Liu, Z. Iron Nanoparticles for Low-Power Local Magnetic Hyperthermia in Combination with Immune Checkpoint Blockade for Systemic Antitumor Therapy. *Nano Lett.* **2019**, 197, 4287-4296
- [37] Zubarev, A. Yu. Magnetic hyperthermia in a system of ferromagnetic particles, frozen in a carrier medium: Effect of interparticle interactions. *Phys. Rev. E.* **2018**, 98, 032610
- [38] Hadadian, Y.; Azimbagirad, M.; Navas, E. A.; Pavan, T. Z. A versatile induction heating system for magnetic hyperthermia studies under different experimental conditions. *Review of Scientific Instruments.* **2019**, 90, 074701
- [39] Usov, N.A.; Nesmeyanov, M.S.; Gubanova, E.M.; Epshtein, N.B. Heating ability of magnetic nanoparticles with cubic and combined anisotropy. *Beilstein J. Nanotechnol.* **2019**, 10, 305–314